Conceptual design of an active feedback system for the control of the resistive shell mode in tokamaks

Richard Fitzpatrick

Citation: Physics of Plasmas (1994-present) **8**, 871 (2001); doi: 10.1063/1.1342783
View online: http://dx.doi.org/10.1063/1.1342783
View Table of Contents: http://scitation.aip.org/content/aip/journal/pop/8/3?ver=pdfcov
Published by the AIP Publishing

Conceptual design of an active feedback system for the control of the resistive shell mode in tokamaks

Richard Fitzpatrick
Institute for Fusion Studies, Department of Physics, University of Texas at Austin, Austin, Texas 78712

(Received 31 August 2000; accepted 12 October 2000)

A quadratic dispersion relation is derived which governs the feedback-modified stability of the resistive shell mode in a large-aspect ratio, low-β tokamak plasma. The effectiveness of a given feedback scheme is determined by a single parameter, α_0, which measures the coupling of different poloidal harmonics due to the nonsinusoidal nature of the feedback currents. Feedback fails when this parameter becomes either too positive or too negative. Feedback schemes can be classified into *three* groups, depending on the relative values of the poloidal mode number, m_0, of the intrinsically unstable resistive shell mode, and the number, M, of feedback coils in the poloidal direction. Group I corresponds to $M \leqslant 2m_0$ and $M \neq m_0$; group II corresponds to $M = m_0$; finally, group III corresponds to $M > 2m_0$. The optimal group I feedback scheme is characterized by extremely narrow detector loops placed as close as possible to the plasma, i.e., well inside the resistive shell. Of course, such a scheme would be somewhat impractical. The optimal group II feedback scheme is characterized by large, nonoverlapping detector loops, and moderately large, nonoverlapping feedback coils. Such a scheme is 100% effective (i.e., it makes the resistive shell appear superconducting) when the detector loops are located just outside the shell. Unfortunately, the scheme only works efficiently for resistive shell modes possessing one particular poloidal mode number. The optimal group III feedback scheme is characterized by slightly overlapping detector loops, and strongly overlapping feedback coils. Such a scheme is 100% effective when the detector loops are located just outside the shell. In addition, the scheme works efficiently for resistive shell modes with a *range* of different poloidal mode numbers. © *2001 American Institute of Physics.* [DOI: 10.1063/1.1342783]

I. INTRODUCTION

The economic attractiveness of magnetic fusion energy is a strongly increasing function of the well-known figure of merit β.[1] Currently, the most promising magnetic fusion concept is the so-called ''advanced tokamak.''[2,3] The maximum achievable β in advanced tokamak designs is limited by pressure gradient driven external-kink modes.[4] Indeed, such designs are only attractive provided that the stability of external-kink modes is enhanced (thus, raising the β limit) via the presence of a close fitting, *perfectly conducting* shell surrounding the plasma. Unfortunately, in a reactor-sized device, all plausible conducting shells possess non-negligible resistivity. When a tokamak plasma is surrounded by a close fitting, *resistive* shell, the relatively fast growing external-kink mode is converted into the far more slowly growing ''resistive shell mode.'' The latter mode grows on the characteristic L/R time of the shell, and has virtually identical stability boundaries to those of the external-kink mode in the absence of a conducting shell.[5] (Rapid plasma rotation can have a stabilizing effect on the resistive shell mode, relative to the free-boundary external-kink mode. Unfortunately, the levels of rotation required to achieve this effect in a reactor-sized device are unrealistically high.[6–8]) The L/R time of a conventional resistive shell is long compared to most plasma time scales, but still generally much shorter than the duration of the plasma discharge. Hence, all attractive advanced tokamak designs are predicated on the assumption that the resistive shell mode can somehow be stabilized.

To date, the only known reactor-relevant mechanism for stabilizing the resistive shell mode in advanced tokamaks is *active feedback* via external saddle coils located outside the shell.[9–15] The subject area of active feedback control of external modes in toroidal pinch devices has matured rapidly over the last decade, starting with Bishop's seminal paper in 1989,[9] and culminating, recently, in the first successful experimental demonstration of feedback control of the resistive shell mode by the (High Beta Tokamak-Extended Pulse) HBT-EP group.[16] Indeed, it now seems highly plausible that the resistive shell mode can be routinely stabilized in an advanced tokamak, given a suitably optimized feedback system.

A typical active feedback system for the control of external modes in a tokamak consists of an array of feedback coils, an array of detector loops, and some electronic circuitry linking the currents driven in the feedback coils to the signals measured by the detector loops. The optimal design of such a system is an extremely complicated procedure, since there are a great many variables, i.e., the nature of the feedback algorithm, the number, sizes, shapes, and locations of the feedback coils, and the number, sizes, shapes, and locations of the detector loops. Fortunately, it is possible to *numerically simulate* a realistic active feedback system by coupling a toroidal (magnetohydrodynamical) MHD stability

code, such as PEST,[17] with a three-dimensional, finite-element, electromagnetic code, such as VALEN,[18] according to a prescription outlined by Boozer.[13] Unfortunately, such simulation is extremely time consuming, effectively precluding a wide-ranging exploration of design parameter space. In this paper, we outline a simple, but highly approximate, *analytic* method—based on low-β, cylindrical MHD analysis—for determining the effectiveness of a given active feedback system. It is hoped that this method can be used to thoroughly explore parameter space in order to identify regions which are sufficiently promising to warrant further investigation via the PEST/VALEN code. Indeed, some of these regions are identified in this paper.

In the current literature, there are two apparently different analytic methods for approximately evaluating the effectiveness of a given active feedback control system in a tokamak. The methods of Boozer[13] and Okabayashi and co-workers[14] emphasize a particular combination of inductances, which in this paper is denoted

$$M_{\rm df}-\frac{M_{\rm dw}M_{\rm wf}}{M_{\rm ww}}. \tag{1}$$

Here, $M_{\rm df}$ measures the mutual inductance between the detector loop array and the feedback coil array, $M_{\rm dw}$ measures the mutual inductance between the detector loop array and the resistive shell, etc. According to Boozer and Okabayashi, if the above-mentioned combination possesses a certain sign (negative in this paper) then the feedback system operates effectively. Conversely, if the combination possesses the opposite sign (positive in this paper) then the feedback system fails. The method of Fitzpatrick and Yu[12] concentrates on a parameter, called α_0 in this paper, which measures the coupling of different poloidal harmonics due to the nonsinusoidal nature of the currents flowing in the feedback coils. According to Fitzpatrick and Yu, effective feedback is only possible provided that α_0 does not exceed a certain critical value. The first aim of this paper is to *unify* the above two approaches to evaluating the effectiveness of a given feedback system.

In a recent paper, Liu and Bondeson obtained a rather surprising result.[15] Namely, in situations where there are only a few feedback coils in the poloidal direction, the optimum configuration is to have *extremely small* detector loops located as close as possible to the edge of the plasma. This result—which is rather perplexing, since extremely small detector loops are likely to have great difficulty sensing low amplitude resistive shell modes—was subsequently confirmed by the PEST/VALEN code.[19] Another aim of this paper is to determine under which circumstances small detector loops are optimal, and whether there are any cases in which practical-sized detector loops are optimal.

The placement of detector loops *well inside* the resistive shell, which appears to be necessary according to the results of Liu and Bondeson, would be highly impractical in a reactor environment. The final aim of this paper is to determine whether or not it is possible to find an optimal feedback system in which the detector loops are located *outside* the resistive shell (which would be far more reactor relevant).

II. DERIVATION OF THE DISPERSION RELATION

A. Introduction

Consider a large aspect-ratio,[20] low-β,[1] tokamak plasma equilibrium whose unperturbed magnetic flux surfaces map out (almost) concentric circles in the poloidal plane. Such an equilibrium is well approximated as a periodic cylinder. Suppose that the minor radius of the plasma is a. Standard cylindrical polar coordinates (r,θ,z) are adopted. The system is assumed to be periodic in the z direction, with periodicity length $2\pi R_0$, where R_0 is the simulated major radius of the plasma. It is convenient to define a simulated toroidal angle $\phi=z/R_0$.

The equilibrium magnetic field is written $\mathbf{B}=[0,B_\theta(r),B_\phi]$. Likewise, the equilibrium plasma current takes the form $\mathbf{J}=[0,0,J_\phi(r)]$, where $\mu_0 J_\phi=(1/r)d(rB_\theta)/dr$. The so-called ''safety factor'' is defined $q=rB_\phi/R_0B_\theta$.

B. Perturbed magnetic field

The perturbed magnetic field can be written $\mathbf{b}=\nabla\psi\wedge\hat{\mathbf{z}}$, where the perturbed poloidal magnetic flux takes the form

$$\psi(r,\theta,\phi,t)=\sum_{m,n}\frac{\psi^{m,n}(r,t)}{m}e^{i(m\theta-n\phi)}. \tag{2}$$

Here, m and n are poloidal and toroidal mode numbers, respectively. The above-given definition is valid provided that $|m|\gg|n|a/R_0$, which is easily satisfied for external-kink modes in a large-aspect ratio tokamak. According to standard, marginally stable, ideal-MHD theory, the function $\psi^{m,n}(r)$ satisfies[21]

$$\frac{1}{r}\frac{d}{dr}\left(r\frac{d\psi^{m,n}}{dr}\right)-\frac{m^2}{r^2}\psi^{m,n}+\frac{\mu_0 J_\phi'}{B_\theta(nq/m-1)}\psi^{m,n}=0, \tag{3}$$

where $(')$ denotes d/dr.

C. Shell physics

Suppose that the plasma is surrounded by a (radially) thin, rigid, concentric, resistive shell of minor radius $r_w>a$. The analysis in this paper is performed in the conventional ''thin shell'' limit, in which the skin depth of the perturbed magnetic field in the shell material is much greater than the thickness of the shell, but much less than its radius. This limit is relevant provided that the thickness of the shell is much less than its minor radius, and the analysis is restricted to cases in which external-kink modes are unstable in the absence of the resistive shell, but stable if the shell is made perfectly conducting.

In the thin shell limit, it is possible to unambiguously define a ''shell flux''

$$\Psi_w(\theta,\phi,t)=\psi(r_w,\theta,\phi,t)=\sum_{m,n}\Psi_w^{m,n}(t)e^{i(m\theta-n\phi)}. \tag{4}$$

Furthermore, the currents induced in the shell have no significant radial variation in this limit. Hence, the radially integrated perturbed shell current density can be written

$$\mu_0 \delta \mathbf{I}_w = i \nabla J_w \wedge \hat{\mathbf{r}}, \tag{5}$$

where

$$J_w(\theta,\phi,t) = \sum_{m,n} J_w^{m,n}(t) e^{i(m\theta - n\phi)} \tag{6}$$

is the shell current stream function. It is helpful to define the quantity

$$\Delta\Psi_w(\theta,\phi,t) = \left[r \frac{\partial \psi(r,\theta,\phi,t)}{\partial r} \right]_{r_{w-}}^{r_{w+}}$$

$$= \sum_{m,n} \Delta\Psi_w^{m,n}(t) e^{i(m\theta - n\phi)}, \tag{7}$$

which parametrizes the jump in the radial derivative of ψ across the shell.

Ampère's law radially integrated across the shell yields

$$\Delta\Psi_w^{m,n} = -m^2 J_w^{m,n}. \tag{8}$$

Finally, Ohm's law combined with Faraday's law gives

$$\Delta\Psi_w^{m,n} = \gamma \tau_w \Psi_w^{m,n}, \tag{9}$$

where $\gamma \equiv d/dt$ is the growth rate, and τ_w is the L/R time of the shell ($\tau_w = \mu_0 \sigma_w \delta_w r_w$, where σ_w is the shell conductivity and δ_w is the shell radial thickness).

D. Feedback coil array

Suppose that the plasma is surrounded by a (radially) thin array of feedback coils of minor radius r_f. Again adopting the thin shell approximation, it is possible to define a ''feedback flux''

$$\Psi_f(\theta,\phi,t) = \psi(r_f,\theta,\phi,t) = \sum_{m,n} \Psi_f^{m,n}(t) e^{i(m\theta - n\phi)}. \tag{10}$$

Moreover, the radially integrated perturbed feedback current density can be written

$$\mu_0 \delta \mathbf{I}_f = i \nabla J_f \wedge \hat{\mathbf{r}}, \tag{11}$$

where

$$J_f(\theta,\phi,t) = \sum_{m,n} J_f^{m,n}(t) e^{i(m\theta - n\phi)} \tag{12}$$

is the feedback current stream function. It is helpful to define the quantity

$$\Delta\Psi_f(\theta,\phi,t) = \left[r \frac{\partial \psi(r,\theta,\phi,t)}{\partial r} \right]_{r_{f-}}^{r_{f+}}$$

$$= \sum_{m,n} \Delta\Psi_f^{m,n}(t) e^{i(m\theta - n\phi)}, \tag{13}$$

which parametrizes the jump in the radial derivative of ψ across the feedback coil array. Ampère's law radially integrated across the array yields

$$\Delta\Psi_f^{m,n} = -m^2 J_f^{m,n}. \tag{14}$$

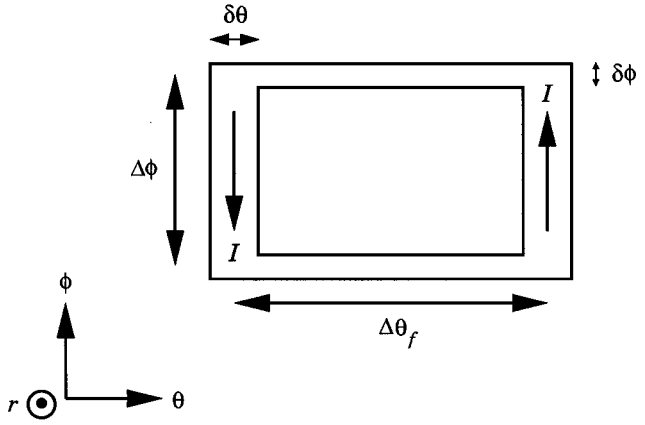

FIG. 1. An individual feedback coil.

E. Feedback coil physics

The distribution of feedback coils is assumed to be toroidally symmetric. It is further assumed that there are sufficient, closely spaced coils in the toroidal direction and that there is negligible coupling of different toroidal harmonics by the feedback currents. Hence, from now on, the common $e^{-in\phi}$ dependence of perturbed quantities is neglected.

Suppose, for the sake of simplicity, that all of the feedback loops are *identical*, and consist of (radially) thin, rectangular, saddle coils, as illustrated in Fig. 1. The poloidal and toroidal angular extents of each coil are $\Delta\theta_f$ and $\Delta\phi$, respectively. Furthermore, the angular widths of the toroidal and poloidal legs of each coil are $\delta\theta$ and $\delta\phi$, respectively. Suppose that there are M coils in the poloidal direction, with the kth coil centered on poloidal angle θ_k.

Let I^k be the total current circulating around the kth coil. For the sake of simplicity, this current is assumed to be *uniformly distributed* throughout the coil. It follows that

$$i J_f^{m,n} = \frac{2\mu_0}{\pi \delta\theta} \frac{\sin(m\delta\theta/2)\sin(m\Delta\theta_f/2)}{m^2} \sum_{k=1,M} I^k e^{-im\theta_k}. \tag{15}$$

The inductive voltage generated in the kth feedback coil takes the form

$$V_i^k = -2iR_0 \Delta\phi \gamma \sum_m \frac{\sin(m\Delta\theta_f/2)}{m} \Psi_f^{m,n} e^{im\theta_k}. \tag{16}$$

F. Detector loop physics

Suppose that each feedback coil is accompanied by a detector loop—centered on the same angular coordinates—located at minor radius r_d. Suppose, further, that all the detector loops are *identical*, (radially) thin, rectangular saddle loops of poloidal and toroidal angular extents $\Delta\theta_d$ and $\Delta\phi$, respectively.

It is possible to define a ''detector flux''

$$\Psi_d(\theta,t) = \psi(r_d,\theta,t) = \sum_{m,n} \Psi_d^{m,n}(t) e^{im\theta}. \tag{17}$$

Moreover, the inductive voltage generated in the kth detector loop takes the form

$$V_d^k = -2iR_0\Delta\phi\gamma\sum_m \frac{\sin(m\Delta\theta_d/2)}{m}\Psi_d^{m,n}e^{im\theta_k}. \tag{18}$$

G. Feedback circuit physics

The circuit equation for the kth feedback coil is written

$$V_i^k + V_f^k = I^k R, \tag{19}$$

where R is the resistance of the coil, and V_f^k is the applied feedback voltage. The feedback algorithm adopted in this paper is similar to that used in the successful HBT-EP experiments.[16] Thus, the feedback voltage V_f^k applied to the kth feedback coil is related to the inductive voltage V_d^k measured by the kth detector loop via

$$V_f^k(t) = G_d V_d^k(t) + G_p\int_{-\infty}^{t} V_d^k(t')\frac{dt'}{\tau_w}, \tag{20}$$

which reduces to

$$V_f^k = \left(G_d + \frac{G_p}{\gamma\tau_w}\right)V_d^k, \tag{21}$$

assuming that the mode amplitude is negligible as $t\rightarrow-\infty$. Here, G_p is termed the *proportional gain*, whereas G_d is termed the *derivative gain*.

H. Inductances

Solving Eq. (3), subject to physical boundary conditions at $r=0$ and $r=\infty$, noting that $\psi^{m,n}(r)$ must be continuous in r but may have gradient discontinuities at $r=r_w$ and $r=r_f$, we obtain

$$\Psi_w^{m,n} = M_{ww}^{m,n}\Delta\Psi_w^{m,n} + M_{wf}^{m,n}\Delta\Psi_f^{m,n}, \tag{22}$$

$$\Psi_f^{m,n} = M_{fw}^{m,n}\Delta\Psi_w^{m,n} + M_{ff}^{m,n}\Delta\Psi_f^{m,n}, \tag{23}$$

$$\Psi_d^{m,n} = M_{dw}^{m,n}\Delta\Psi_w^{m,n} + M_{df}^{m,n}\Delta\Psi_f^{m,n}. \tag{24}$$

Here,

$$M_{ww}^{m,n} = \frac{1}{2|m|}\frac{r_m^{2|m|}-r_w^{2|m|}}{r_w^{2|m|}}, \tag{25}$$

$$M_{ff}^{m,n} = \frac{1}{2|m|}\frac{r_m^{2|m|}-r_f^{2|m|}}{r_f^{2|m|}}, \tag{26}$$

$$M_{fw}^{m,n} = M_{wf}^{m,n} = \frac{1}{2|m|}\frac{r_m^{2|m|}-r_{fw}^{2|m|}}{r_f^{|m|}r_w^{|m|}}, \tag{27}$$

$$M_{dw}^{m,n} = \frac{1}{2|m|}\frac{r_m^{2|m|}-r_{dw}^{2|m|}}{r_d^{|m|}r_w^{|m|}}, \tag{28}$$

$$M_{df}^{m,n} = \frac{1}{2|m|}\frac{r_m^{2|m|}-r_{df}^{2|m|}}{r_d^{|m|}r_f^{|m|}}, \tag{29}$$

where

$$r_{fw} = \min(r_f, r_w), \tag{30}$$

$$r_{dw} = \min(r_d, r_w), \tag{31}$$

$$r_{df} = \min(r_d, r_f). \tag{32}$$

The quantity r_m is termed the *critical radius* for the m,n ideal external-kink mode: a resistive shell whose minor radius exceeds r_m is incapable of stabilizing the mode, and *vice versa*.

The quantities $M_{ww}^{m,n}$, $M_{wf}^{m,n}$, etc., can all be interpreted as *normalized inductances* (the true inductances are obtained by multiplying by $-\mu_0 R_0$). Thus, $M_{ww}^{m,n}$ measures the self-inductance of the current distribution associated with the m,n resistive shell mode, assuming the presence of a single resistive shell at radius r_w, and no feedback. Likewise, $M_{ff}^{m,n}$ measures the self-inductance of the current distribution associated with the m,n resistive shell mode, assuming the presence of a single resistive shell at radius r_f, and no feedback. Furthermore, $M_{fw}^{m,n}$ measures the mutual inductance between these two current distributions. Finally, $M_{dw}^{m,n}$ and $M_{df}^{m,n}$ measure the mutual inductance between the detector loop array and the former and latter current distributions, respectively.

I. Dispersion relation

In general, for physically plausible tokamak current profiles, at most *one* resistive shell mode—the m_0, n mode, say—is intrinsically unstable at any given time.[22] The intrinsically unstable m_0, n harmonic is termed the ''central harmonic.''

Suppose that the feedback coils are evenly spaced, so that

$$\theta_k = (k-1)\frac{2\pi}{M} \tag{33}$$

for $k=1,M$. In this case, only the

$$m = m_0 + jM \tag{34}$$

(where j is an integer) harmonics need be included in the calculation of the feedback modified growth rate of the intrinsically unstable m_0, n resistive shell mode. Following the analysis of Ref. 12, we write

$$I^k = Ie^{im_0\theta_k}. \tag{35}$$

Equations (8), (9), (14)–(16), (18), (19), (21)–(24), and (35) can be combined to give the following dispersion relation:

$$\sum_{j,m\neq 0}^{m=m_0+jM}\gamma\tau_f\left\{g_f(m,m_0)\left(\frac{\gamma\tau_w M_{fw}^m M_{wf}^m}{1-\gamma\tau_w M_{ww}^m}+M_{ff}^m\right)+g_d(m,m_0)\times\left(\frac{\gamma\tau_w M_{dw}^m M_{wf}^m}{1-\gamma\tau_w M_{ww}^m}+M_{df}^m\right)\left(G_d+\frac{G_p}{\gamma\tau_w}\right)\right\}=1, \tag{36}$$

where

$$\tau_f = \frac{\mu_0 R_0}{R}\frac{4M\Delta\phi}{\pi\delta\theta}\frac{\sin(m_0\delta\theta/2)\sin^2(m_0\Delta\theta_f/2)}{m_0} \tag{37}$$

is the L/R time of the feedback coil array, and

$$g_f(m,m_0) = \frac{m_0\sin(m\delta\theta/2)\sin^2(m\Delta\theta_f/2)}{m\sin(m_0\delta\theta/2)\sin^2(m_0\Delta\theta_f/2)}, \tag{38}$$

$$g_d(m,m_0)=\frac{m_0\sin(m\delta\theta/2)\sin(m\Delta\theta_f/2)\sin(m\Delta\theta_d/2)}{m\sin(m_0\delta\theta/2)\sin^2(m_0\Delta\theta_f/2)}. \tag{39}$$

Note that the common superscript n on the inductances has been omitted for the sake of clarity.

Let us assume, as seems reasonable, that the L/R time of the resistive shell greatly exceeds that of the feedback coil array, i.e.,

$$\tau_w \gg \tau_f. \tag{40}$$

For the case of resistive shell modes (i.e., modes for which $1/\tau_f \gg \gamma \sim 1/\tau_w$), the above-mentioned dispersion relation reduces to

$$\hat{\gamma}^2[(\alpha-\tilde{\alpha}_{\min})\hat{G}_d]+\hat{\gamma}[1+(\alpha-\tilde{\alpha}_{\min})\hat{G}_p +(\alpha_{\max}-\alpha)s\hat{G}_d]+[(\alpha_{\max}-\alpha)s\hat{G}_p-s]=0, \tag{41}$$

where

$$\hat{\gamma}=\frac{\gamma\tau_w}{2m_0}, \tag{42}$$

$$\hat{G}_d=\frac{\tau_f}{\tau_w}g_d(m_0,m_0)G_d, \tag{43}$$

$$\hat{G}_p=\frac{\tau_f}{\tau_w}g_d(m_0,m_0)\frac{G_p}{2m_0}, \tag{44}$$

$$s=\frac{1}{2m_0M_{ww}^{m_0}}=\frac{r_w^{2m_0}}{r_{m_0}^{2m_0}-r_w^{2m_0}}, \tag{45}$$

$$\alpha_{\max}=2m_0M_{df}^{m_0}=\frac{r_{m_0}^{2m_0}-r_{df}^{2m_0}}{r_d^{m_0}r_f^{m_0}}, \tag{46}$$

$$\tilde{\alpha}_{\min}=2m_0\left(M_{df}^{m_0}-\frac{M_{dw}^{m_0}M_{wf}^{m_0}}{M_{ww}^{m_0}}\right) =\frac{1}{r_d^{m_0}r_f^{m_0}}\left\{(r_{m_0}^{2m_0}-r_{df}^{2m_0}) -\frac{(r_{m_0}^{2m_0}-r_{dw}^{2m_0})(r_{m_0}^{2m_0}-r_{fw}^{2m_0})}{(r_{m_0}^{2m_0}-r_w^{2m_0})}\right\}, \tag{47}$$

$$\alpha=-\sum_{j,j\neq 0,m\neq 0}^{m=m_0+jM}\frac{g_d(m,m_0)}{g_d(m_0,m_0)} \times\left[\frac{\hat{\gamma}(2m_0)^2M_{dw}^mM_{wf}^m}{1-\hat{\gamma}2m_0M_{ww}^m}+2m_0M_{df}^m\right]. \tag{48}$$

III. DERIVATION OF THE REDUCED DISPERSION RELATION

A. Introduction

Let us, first of all, examine the various quantities appearing in the dispersion relation (41). The quantities $\hat{\gamma}$, $\hat{G}_p$, $\hat{G}_d$ are the normalized growth rate, proportional gain, and derivative gain, respectively. The quantity s measures the intrinsic stability of the m_0, n resistive shell mode. If $s>0$ then the mode is unstable. The associated ideal external-kink mode becomes unstable as $s\to\infty$. Now, the analysis in this paper is premised on the assumption that the m_0, n resistive shell mode is *unstable* and the associated ideal external-kink mode is *stable*. Hence, we shall restrict our attention to cases in which $0<s<\infty$. The quantity α measures the coupling of the central harmonic to sideband harmonics (i.e., harmonics with $m\neq m_0$) due to the nonsinusoidal nature of the currents flowing in the feedback coils. The interpretations of the quantities $\tilde{\alpha}_{\min}$ and $\alpha_{\max}$ will become clearer presently.

B. Feedback mode

In this paper, we assume that both $\hat{G}_p$ and $\hat{G}_d$ are *positive*, which corresponds (under normal circumstances) to negative feedback applied to the resistive shell mode. We also assume, for the moment, that the derivative gain, $\hat{G}_d$, is much less than unity. In this limit, the dispersion relation (41) can be split into two separate branches. The first branch corresponds to a fast-growing mode whose growth rate is inversely proportional to $\hat{G}_d$:

$$\hat{\gamma}\simeq\left[\frac{1}{\tilde{\alpha}_{\min}-\alpha_\infty}-\hat{G}_p\right]\Big/\hat{G}_d. \tag{49}$$

Here

$$\alpha_\infty=\lim_{\gamma\to\infty}\alpha. \tag{50}$$

Note that the above-mentioned growth rate is *independent* of the plasma stability parameter, s. This suggests that the corresponding mode represents an instability of the feedback system, rather than the plasma: Hence, it is termed the *feedback mode*.

According to Eq. (49), the feedback mode is intrinsically unstable whenever

$$\alpha_\infty<\tilde{\alpha}_{\min}, \tag{51}$$

but is stabilized by proportional gain. Indeed, the critical value of $\hat{G}_p$ above which the mode is stabilized is

$$\hat{G}_{pf}=\frac{1}{\tilde{\alpha}_{\min}-\alpha_\infty}. \tag{52}$$

As $\hat{G}_d\to 0$, the growth rate of the feedback mode increases monotonically until $\hat{\gamma}\sim 1/\tau_f$, at which point the mode drops out of the dispersion relation (41), which is restricted to modes whose growth rates are much smaller than $1/\tau_f$.

C. Resistive shell mode

The second branch of the dispersion relation (41) corresponds to a mode which grows on the inverse L/R time of the shell, and whose growth rate becomes very large as the ideal stability boundary $s=\infty$ is approached:

$$\hat{\gamma}\simeq\frac{s[1-(\alpha_{\max}-\alpha)\hat{G}_p]}{[1+(\alpha-\tilde{\alpha}_{\min})\hat{G}_p]}. \tag{53}$$

Of course, we immediately recognize this branch as the *resistive shell mode*.

Expression (53) exhibits *three* different regimes of behavior as the proportional gain, $\hat{G}_p$, is increased from a small value, depending on the size of the mode coupling parameter, α.

If

$$\alpha_0 > \alpha_{\max}, \tag{54}$$

where

$$\alpha_0 = \lim_{\gamma \to 0} \alpha, \tag{55}$$

then as $\hat{G}_p$ is increased the mode growth rate is reduced, but never becomes negative. In other words, in this regime the feedback system is incapable of completely stabilizing the resistive shell mode. This behavior is similar to that described in Fitzpatrick and Yu (1998).[12] Excessive coupling to sideband harmonics (parametrized by α_0) causes the structure of the resistive shell mode eigenfunction to *distort* strongly under the influence of the feedback currents, leading eventually to the escape of the mode through the gaps between the feedback coils, or the centers of the coils.

If

$$\alpha_0 < \alpha_{\max}, \tag{56}$$

and

$$\alpha_\infty > \tilde{\alpha}_{\min}, \tag{57}$$

then the resistive shell mode is stabilized once the proportional gain exceeds the critical value

$$\hat{G}_{pw} = \frac{1}{\alpha_{\max} - \alpha_0}. \tag{58}$$

Hence, in this regime the feedback system operates effectively.

Finally, if

$$\alpha_\infty < \tilde{\alpha}_{\min}, \tag{59}$$

then the resistive shell mode is stabilized once $\hat{G}_p$ exceeds the critical value (58), but becomes unstable again when $\hat{G}_p$ exceeds the second critical value (52). Note, however, that for $\hat{G}_p$ less than the second critical value the feedback mode is unstable (see Sec. III B). Hence, there is an unstable mode for *all* (positive) values of the proportional gain. Clearly, the feedback system fails completely in this regime.

D. Reduced dispersion relation

At first sight, the dispersion relation (41) appears to be a quadratic equation for the growth rate, $\hat{\gamma}$. This is, in fact, not the case because of the hidden $\hat{\gamma}$ dependence of the mode coupling parameter, α. Consider the modified dispersion relation

$$\hat{\gamma}^2[(\alpha_\infty - \tilde{\alpha}_{\min})\hat{G}_d] + \hat{\gamma}[1 + (\alpha_\infty - \tilde{\alpha}_{\min})\hat{G}_p + (\alpha_{\max} - \alpha_0)s\hat{G}_d] + [(\alpha_{\max} - \alpha_0)s\hat{G}_p - s] = 0. \tag{60}$$

This is a true quadratic equation for $\hat{\gamma}$, since the parameters α_0 and α_∞ are $\hat{\gamma}$ independent. The condition for both roots of Eq. (60) to remain negative is simply that all coefficients of $\hat{\gamma}^n$ remain the same sign. In fact, following Boozer (1998),[13] if a finite time delay is incorporated into the analysis of the feedback circuits then the stability condition becomes slightly more stringent: namely, that all coefficients remain *positive*. It follows that if $s > 0$, $\hat{G}_d > 0$, and $\hat{G}_p \gg 1$, which corresponds to the normal operating regime of our feedback scheme, then both roots of Eq. (60) are stable provided that $\alpha_{\max} > \alpha_0$ and $\alpha_\infty > \tilde{\alpha}_{\min}$. Of course, these stability boundaries are identical to those we have just derived for the true dispersion relation (41). We conclude that, as long as we are only interested in whether modes are stable or unstable, rather than their exact growth rates, it is sufficient to consider the simple quadratic dispersion relation (60), rather than the full dispersion relation (41).

The reduced dispersion relation (60) can be rewritten

$$\hat{\gamma}^2[(\alpha_0 - \alpha_{\min})\hat{G}_d] + \hat{\gamma}[1 + (\alpha_0 - \alpha_{\min})\hat{G}_p + (\alpha_{\max} - \alpha_0)s\hat{G}_d] + [(\alpha_{\max} - \alpha_0)s\hat{G}_p - s] = 0, \tag{61}$$

where

$$\alpha_{\min} = \tilde{\alpha}_{\min} + \alpha_0 - \alpha_\infty. \tag{62}$$

The stability criterion, in the limit of large proportional gain (i.e., $\hat{G}_p \gg 1$), becomes

$$\alpha_{\max} > \alpha_0 > \alpha_{\min}. \tag{63}$$

In other words, the mode coupling parameter, α_0, is constrained to lie within a certain *band* of values. If α_0 crosses the upper boundary of this band (from below) then mode coupling becomes sufficiently strong that the distortion of the resistive shell mode eigenfunction under the influence of the feedback currents defeats the feedback scheme. Conversely, if α_0 crosses the lower boundary of the band (from above) then the feedback scheme itself becomes unstable.

E. Evaluation of mode coupling parameters

In order to solve the reduced dispersion relation (61) we need to derive expressions for the mode coupling parameters α_0 and α_∞, defined in Eqs. (55) and (50), respectively. For the sake of simplicity, let us adopt a *vacuum approximation* in which the interactions of the various sideband harmonics with the plasma are assumed to be negligible. This is equivalent to taking the limit $r_m \to 0$ (recall that r_m is the critical radius for the m, n ideal external-kink mode) for all m, n harmonics except the central harmonic. Let us also neglect the thickness of the feedback coil conductors, which is equivalent to taking the limit $\delta\theta \to 0$. In these limits, Eqs. (48), (50), and (55) yield

$$\alpha_0 = \sum_{j, j \neq 0, m \neq 0}^{m = m_0 + jM} \left(\frac{r_{df}^2}{r_d r_f} \right)^{|m|} \frac{m_0}{|m|} \frac{\sin(m\Delta\theta_f/2)\sin(m\Delta\theta_d/2)}{\sin(m_0\Delta\theta_f/2)\sin(m_0\Delta\theta_d/2)}, \tag{64}$$

and

$$\alpha_\infty = \sum_{j,j\neq 0,m\neq 0}^{m=m_0+jM} \left(\frac{r_{df}^2}{r_d r_f}\right)^{|m|}\left[1-\left(\frac{r_{dw}r_{fw}}{r_{df}r_w}\right)^{2|m|}\right] \times \frac{m_0}{|m|}\frac{\sin(m\Delta\theta_f/2)\sin(m\Delta\theta_d/2)}{\sin(m_0\Delta\theta_f/2)\sin(m_0\Delta\theta_d/2)}. \quad (65)$$

F. Discussion

It is appropriate, at this point, to list the assumptions made during the derivation of the reduced dispersion relation (61): (1) The plasma equilibrium configuration corresponds to a large aspect-ratio, low-β tokamak. (2) The plasma is surrounded by a single, concentric, (radially) thin, resistive shell. (3) The feedback system consists of a concentric array of (radially) thin feedback coils and a concentric array of (radially) thin detector loops, both located outside the plasma. (4) There are sufficient feedback coils in toroidal direction to prevent the coupling of different toroidal harmonics by the feedback currents. (5) Each feedback coil is accompanied by an associated detector loop. (6) The feedback coils are evenly spaced in the poloidal direction. (7) Each detector loop is centered on the same angular position as its associated feedback coil. However, the radial locations of the detector loop and feedback coil arrays are not necessarily the same. (8) All feedback coils are identical rectangular saddle coils. All detector loops are identical rectangular saddle loops. (9) The feedback coils and detector loops are the same size in the toroidal direction. However, the detector loops and feedback coils may be different sizes in the poloidal direction. (10) There is only a single intrinsically unstable resistive shell mode, known as the ''principal harmonic.'' (11) All harmonics other than the principal harmonic are treated via a vacuum approximation in which their interaction with the plasma is neglected. (12) The angular widths of the conductors making up the feedback coils are negligible. (13) The L/R time of the resistive shell greatly exceeds that of the feedback coil array. (14) An identical feedback algorithm is applied *independently* to each detector loop/feedback coil pair.

The parameters appearing in Eq. (61) are as follows:

(1) $\hat{\gamma}$ is the normalized growth-rate, defined in Eq. (42);
(2) $\hat{G}_p$ is the normalized proportional gain, defined in Eqs. (21) and (44);
(3) $\hat{G}_d$ is the normalized derivative gain, defined in Eqs. (21) and (43);
(4) s is the plasma stability parameter, defined in Eq. (45);
(5) α_0 is the mode coupling parameter, defined in Eq. (64);
(6) $\alpha_{\max}$, defined in Eq. (46), is the maximum value of α_0 at which the feedback scheme still operates effectively; and
(7) $\alpha_{\min}$, defined in Eqs. (47), (62), (64), and (65), is the minimum value of α_0 at which the feedback scheme still operates effectively.

Note that the purpose of the reduced dispersion relation (61) is merely to predict whether the growth-rate $\hat{\gamma}$ is positive or negative. The full dispersion relation (41) must be used to obtain an accurate estimate for $\hat{\gamma}$.

The stability criteria specified in Eq. (63) can be related to previously published criteria. For instance, the criterion $\alpha_{\max} > \alpha_0$ is identical to that of Fitzpatrick and Yu (1998).[12] Moreover, the criterion $\alpha_0 > \alpha_{\min}$ can be related to that of Boozer (1998)[13] and Okabayashi, Pomphrey, and Hatcher (1998).[14] Note that the latter two criteria were obtained from *single harmonic* calculations in which the effects of sideband harmonics were completely neglected. In the single harmonic limit, it is easily seen that $\alpha_0 = \alpha_\infty = 0$. Thus, the $\alpha_0 > \alpha_{\min}$ criterion reduces to $0 > \overline{\alpha}_{\min}$. According to Eq. (47), this reduced criterion can be written

$$M_{df}^{m_0} - \frac{M_{dw}^{m_0} M_{wf}^{m_0}}{M_{ww}^{m_0}} < 0, \quad (66)$$

which is identical in form to the criteria of Boozer and Okabayashi. It can be seen, from Eqs. (22) to (24), that the above-mentioned combination of inductances represents the normalized mutual inductance between the feedback coil and detector loop arrays associated with the m_0, n, marginally stable, ideal external-kink eigenfunction (i.e., the marginally stable eigenfunction which satisfies $\Psi_w^{m_0,n} = 0$). If this inductance is negative (which implies that the unnormalized inductance is positive) then the feedback scheme is intrinsically stable. Conversely, if the inductance is positive then the feedback scheme becomes unstable.

IV. OPTIMAL DESIGN OF THE FEEDBACK SYSTEM

A. Introduction

In the following, we employ the quadratic dispersion relation (61) to optimize the design of our feedback system. A given system is fully described once the values of the following *ten* physics parameters are specified:

(1) m_0—the poloidal mode number of the intrinsically unstable m_0, n resistive shell mode;
(2) M—the number of evenly spaced feedback coil/detector loop pairs in the poloidal direction;
(3) $\Delta\theta_f$—the poloidal angular extent of each feedback coil;
(4) $\Delta\theta_d$—the poloidal angular extent of each detector loop;
(5) r_{m_0}—the critical (minor) radius beyond which a resistive shell is unable to stabilize the m_0, n ideal external-kink mode;
(6) r_w—the (minor) radius of the resistive shell;
(7) r_f—the (minor) radius of the feedback coil array;
(8) r_d—the (minor) radius of the detector loop array;
(9) $\hat{G}_p$—the normalized proportional gain; and
(10) G_d—the normalized derivative gain.

The necessary constraint that the m_0, n ideal external-kink mode be stable implies that $r_{m_0} > r_w$. Otherwise, the above ten parameters are free to take *any* (physically plausible) values.

Our present study concentrates on the stability of a low-m external kink-mode (i.e., $m_0 = 3$), moderated by a relatively close-fitting resistive shell (i.e., $r_w = 1.1a$), which is surrounded by a fairly close-fitting array of feedback coils (i.e., $r_f = 1.2a$), since these choices are particularly relevant to present-day tokamak experiments.[16] The derivative gain is

set to a small, positive, constant value (i.e., $\hat{G}_d=0.01$): This allows the dispersion relation (61) to monitor instabilities of the feedback system, whilst ensuring that all meaningful feedback of the m_0, n resistive shell mode is due to proportional gain (which is the only effective type of feedback, anyway, given the orderings adopted in this paper). It follows that only *six* of the above-mentioned physics parameters (i.e., M, $\Delta\theta_f$, $\Delta\theta_d$, r_{m_0}, r_d, and $\hat{G}_p$) are actually varied during our design study.

B. Effective radius

In order to optimize the design of our feedback system, we must first select a *meaningful* figure of merit. Past experience has demonstrated that the feedback gain, $\hat{G}_p$, is *not* a particularly meaningful figure, i.e., the feedback scheme which operates effectively with the lowest value of $\hat{G}_p$ is not necessarily the optimal scheme. Without doubt, the best figure of merit is the so-called *effective radius*. By definition, a feedback scheme with a given effective radius—r_e, say—has the same stabilizing effect on the m_0, n mode as a *perfectly conducting* shell of minor radius r_e. The type of feedback scheme considered in this paper always has an effective radius greater than or equal to the radius, r_w, of the resistive shell, i.e., the best the scheme can do is to make the resistive shell appear superconducting—it cannot make the shell appear closer to the plasma than is actually the case. Thus, an optimal feedback scheme corresponds to one in which the effective radius is made as close as possible to the actual radius of the shell.

As is easily demonstrated, in the *absence* of mode coupling (i.e., $\alpha_0=\alpha_\infty=0$), the effective radius is determined from the relation $\alpha_{\max}=0$ (subject to the constraint $r_{m_0}>r_w$). It follows, from Eqs. (45) and (46), that

$$r_e=\max(r_w,r_{df}) \tag{67}$$

in this simple limit. In other words, if r_d exceeds r_f then the effective radius is r_f; if r_d lies between r_w and r_f then the effective radius is r_d; and if r_d is less than r_w then the effective radius is r_w. This implies that the optimum location for the detector loop array is just outside the resistive shell: in this case, $r_e=r_w$. In particular, there is no benefit in placing the detector loop array inside the shell.

In the *presence* of mode coupling, the effective radius corresponds to the lowest value of r_{m_0} for which neither the Fitzpatrick–Yu stability criterion, $\alpha_0<\alpha_{\max}$, nor the Boozer–Okabayashi stability criterion, $\alpha_0>\alpha_{\min}$, are violated (subject to the constraint $r_{m_0}>r_w$). In practice, the effective radius is calculated by setting the proportional gain to a large positive value (i.e., $\hat{G}_p=10^6$), and then gradually reducing the critical radius, r_{m_0}, from infinity, until the dispersion relation (61) predicts a positive growth rate. The value of r_{m_0} at which this occurs is essentially identical to the effective radius. In the following, we shall search $\{M,\Delta\theta_f,\Delta\theta_d,r_d\}$ parameter space for regions in which the effective radius is minimized. Such regions invariably correspond to regions in which the mode coupling parameter, α_0, lies close to zero.

As can be seen from Eq. (64), α_0 depends only on the properties of the feedback coil and detector loop arrays. In fact, there are *three* main factors which affect the amplitude of this parameter. First, if $\Delta\theta_f-\Delta\theta_d$ is nonzero (i.e., if the feedback coils and detector loops are of different angular sizes) then the sign of the terms appearing in the summation in Eq. (64) can oscillate, leading to cancellation. On the other hand, if $\Delta\theta_f=\Delta\theta_d$ then every term is positive definite. It follows that mode coupling is maximized when the feedback coils and detector loops are of the same angular size. Hence, an optimal feedback scheme will almost certainly have feedback coils and detector loops of *different* angular sizes. Second, as the radial distance, $|r_f-r_d|$, between the feedback coils and the detector loops increases, the amplitude of α_0 generally decreases. It follows that an optimal feedback scheme will probably have a *finite gap* between the feedback coils and the detector loops. Finally, as the number, M, of feedback coil/detector loop pairs in the poloidal direction increases, the amplitude of α_0 tends to decrease. Hence, finding a robust low-M optimal feedback scheme is likely to pose a challenge.

C. Feedback efficacy parameter

Suppose that the m_0, n resistive shell mode is driven unstable by pressure gradients within the plasma. Let $\beta_{\rm nw}$ be the β limit calculated in the absence of the resistive shell (i.e., the ''no-wall'' β limit), and let $\beta_{\rm pw}$ be the β limit calculated assuming that the shell acts like a perfect conductor (i.e., the ''perfect-wall'' β limit). We expect the following approximate β dependence of the plasma stability parameter, s:

$$s\simeq\frac{\beta-\beta_{\rm nw}}{\beta_{\rm pw}-\beta}. \tag{68}$$

In other words, we expect s to pass through zero and become positive as the no-wall β limit is exceeded, and to become infinite as the perfect-wall β limit is approached.

Let s_c and β_c be the critical values of the plasma stability parameter and the plasma β, respectively, above which the m_0, n resistive shell mode becomes unstable when the feedback system is in operation. The relationship between s_c and the effective radius, r_e, of the feedback system is simply [see Eq. (45)]

$$s_c=\frac{r_w^{2m_0}}{r_e^{2m_0}-r_w^{2m_0}}. \tag{69}$$

It is helpful to define the *feedback efficacy parameter*:

$$\kappa=\frac{\beta_c-\beta_{\rm nw}}{\beta_{\rm pw}-\beta_{\rm nw}}. \tag{70}$$

If $\kappa=0$ then the feedback system is *completely ineffective*: In other words, the β limit is the same as that calculated in the absence of a resistive shell. If $\kappa=1$ then the feedback system is *completely effective*: In other words, the β limit is the same as that calculated assuming that the shell behaves like a perfect conductor. Finally, if $0<\kappa<1$ then the feedback system is partially effective: For instance, if $\kappa=0.5$ then the

feedback modified β limit lies halfway between the no-wall and perfect-wall β limits. It is easily demonstrated, from Eqs. (68) to (70), that the relationship between the feedback efficacy parameter, κ, and the effective radius, r_e, is simply

$$\kappa = \left(\frac{r_e}{r_w}\right)^{2m_0}. \tag{71}$$

D. Results

Extensive exploration of $\{M, \Delta\theta_f, \Delta\theta_d, r_d\}$ parameter space reveals the existence of *three* distinct regions, depending on the size of M. Region I corresponds to $M \leqslant 2m_0$, but $M \neq m_0$. Region II corresponds to $M = m_0$. Finally, region III corresponds to $M > 2m_0$. In the following, each of these regions is described in detail.

E. Region I: $M \leqslant 2m_0$, $M \neq m_0$

The fundamental design philosophy adopted in this paper is to attempt to set the mode coupling parameter, α_0, to zero when the radius of the detector loop array is equal to that of the resistive shell (i.e., when $r_d = r_w$). It turns out that this is impossible in region I: The best we can achieve is to *minimize* α_0.

Figure 2(a) shows the loci of all points in $\Delta\theta_d - \Delta\theta_f$ parameter space at which α_0 is a local minimum, calculated for an example case in which $M=1$ and $m_0=3$. There are two mirror-image curves: the first corresponding to a branch of semioptimal feedback schemes on which the detector loops are *wider* than the feedback coils, and the second to a branch on which the detector loops are *narrower* than the feedback coils. As expected, there are no semioptimal schemes for which the detector loops and feedback coils are the same size. Figure 2(b) shows the local minimum value of α_0 on the second branch, plotted as a function of $\Delta\theta_d$ (note, the local minimum value is identical on the other branch). It can be seen that the mode coupling parameter rises rapidly as the width of the detector loops increases. Hence, the optimal design (i.e., the design which absolutely minimizes α_0) corresponds to one in which the detector loops are *extremely small*. This result is in accordance with the numerical simulations of Liu and Bondeson (2000).[15]

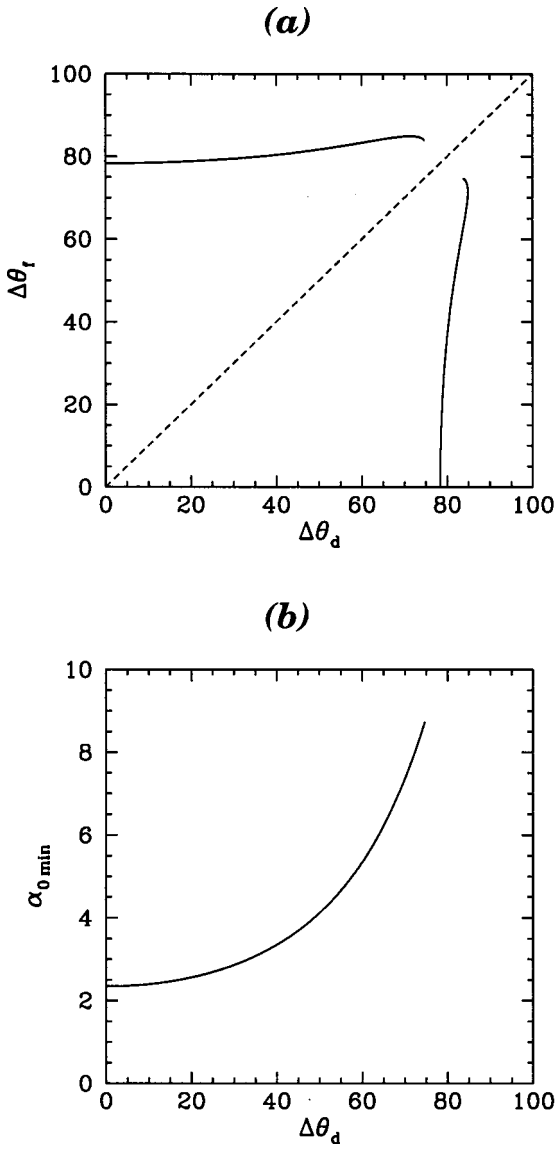

FIG. 2. (a) Values of $\Delta\theta_f$ and $\Delta\theta_d$ (in deg) which locally minimize α_0, calculated with $M=1$, $m_0=3$, $r_w=1.1a$, and $r_f=1.2a$. (b) The local minimum value of α_0 on the $\Delta\theta_d < \Delta\theta_f$ branch of (a), plotted as a function of $\Delta\theta_d$.

Figure 3(a) shows the mode coupling parameter, α_0, plotted as a function of the detector array radius, r_d, for the optimal $M=1$ feedback scheme—which corresponds to $\Delta\theta_d = 1°$ and $\Delta\theta_f = 78.3°$ (i.e., extremely narrow detector loops, and fairly wide feedback coils). As expected, α_0 peaks when $r_d = r_f$, suggesting that a feedback scheme in which the detector loops are located very close to the feedback coils is likely to operate relatively ineffectively. Note that α_0 rises above $\alpha_{\max}$ at large r_d, which implies that the feedback scheme fails to operate effectively when the detector loops are located too far from the plasma. Note, finally, that $\alpha_0 = \alpha_{\min}$ for $r_d < r_f$. This is a general result. It turns out that $\alpha_0 = \alpha_{\min}$ in any case where the feedback coils and detector loops are located on *opposite sides* of the shell—thus, automatically precluding violation of the Boozer–Okabayashi stability criterion (i.e., $\alpha_0 < \alpha_{\min}$). This behavior makes physical sense because violation of the Boozer–Okabayashi criterion entails the appearance of a fast growing instability (i.e., $\gamma \gg 1/\tau_w$), driven by inductive coupling between the feedback coils and detector loops. Of course, when the feedback coils and detector loops are located on opposite sides of the shell they are shielded from one another—at least as far as fast growing modes are concerned. Hence, there is no inductive coupling, and, thus, no instability is possible.

Figure 3(b) shows the feedback efficacy parameter, κ, plotted as a function of the detector array radius, r_d, for the optimal $M=1$ feedback scheme illustrated in Fig. 3(a). It can be seen that κ is rather small (far smaller, for instance, than the corresponding parameter calculated in the absence of mode coupling—as is clear from the figure), reflecting the relatively high values of α_0 shown in Fig. 3(a). The largest value of κ is obtained when $r_d = a$.

We conclude that, with only a single feedback coil in the poloidal direction, the optimal feedback scheme corresponds

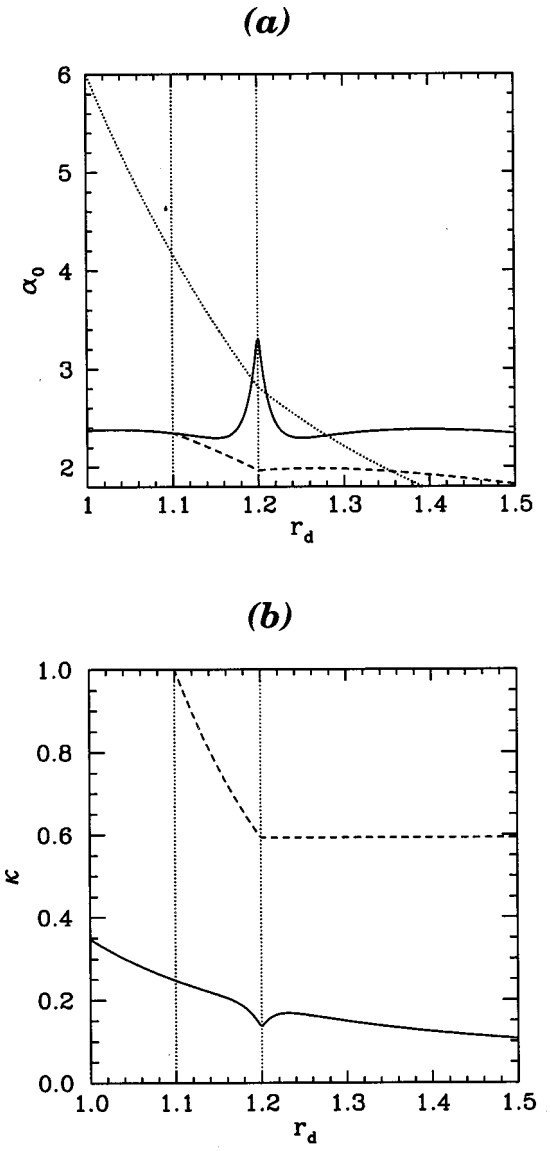

FIG. 3. (a) Values of α_0 (solid curve), $\alpha_{\max}$ (dotted curve), and $\alpha_{\min}$ (dashed curve), plotted as a function of r_d (divided by a), for $\Delta\theta_d=1°$, $\Delta\theta_f=78.3°$, $M=1$, $m_0=3$, $r_{m_0}=1.5a$, $r_w=1.1a$, and $r_f=1.2a$. The locations of the shell and the feedback coil array are indicated by vertical dotted lines. (b) The feedback efficacy parameter, κ, plotted as a function of r_d, for the same parameters as in (a). The dashed curve shows the κ vs r_d relation calculated assuming zero mode coupling.

to one with moderately large feedback coils (i.e., $\Delta\theta_f\sim 70°$), and very small detector loops placed as close to the plasma as possible. However, such a scheme performs relatively poorly, since its feedback efficacy parameter is significantly less than unity (i.e., $\kappa<0.35$, which implies that the feedback-modified β limit is less than 35% of the way between the no-wall and perfect-wall β limits). These conclusions are in complete accordance with those of Liu and Bondeson (2000).[15]

Note, incidentally, that, since α_0 is invariant under the transformation $\Delta\theta_f\leftrightarrow\Delta\theta_d$ [see Eq. (64)], the widths of the feedback coils and detector loops can be *interchanged* in any optimal feedback scheme, without affecting the scheme's performance. Thus, an alternative, optimal, $M=1$ feedback

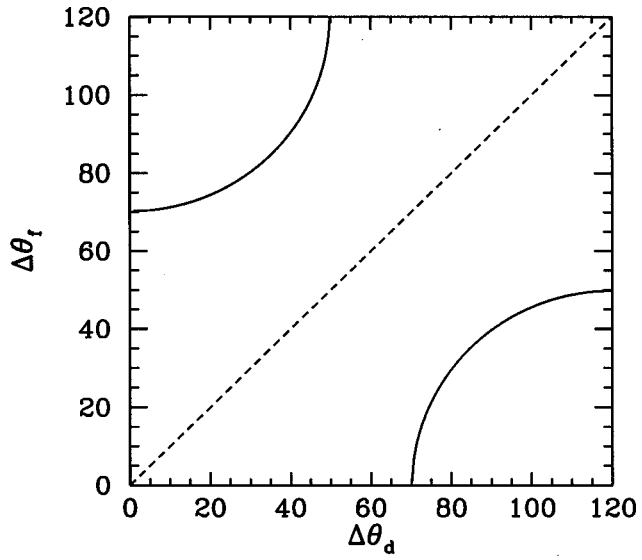

FIG. 4. Values of $\Delta\theta_f$ and $\Delta\theta_d$ (in deg) for which $\alpha_0=0$, calculated with $M=3$, $m_0=3$, $r_w=1.1a$, and $r_f=1.2a$.

scheme consists of very small feedback coils, and moderately large detector loops (i.e., $\Delta\theta_d\sim 70°$) placed as close to the plasma as possible. Of course, such a scheme would be extremely impractical.

The above-noted conclusion (i.e., that the optimal scheme corresponds to very small detector loops placed well inside the shell) remains valid for all other values of M which fall within region I. In general, the performance of the scheme improves (i.e., κ increases) as M increases. However, no region I feedback scheme performs particularly well.

F. Region II: $M=m_0$

In region II, it is actually possible to set the mode coupling parameter, α_0, to zero when $r_d=r_w$. The main difference between regions I and II is that, in the latter case, $m=0$ is one of the nearest-neighbor sideband harmonics. Now, the $m=0$ harmonic does not couple to resistive shell modes in a large aspect-ratio, low-β, tokamak, so one of the nearest-neighbor terms in the summation (64) is *absent* in region II. Since nearest-neighbor terms are relatively large, and invariably positive, it follows that α_0 is significantly less positive in region II than in region I. Thus, it is not particularly surprising that, although α_0 is always positive in region I, it can be made negative (or zero) in region II.

Figure 4 shows the loci of all points in $\Delta\theta_d-\Delta\theta_f$ parameter space at which $\alpha_0=0$, calculated for an example case in which $M=3$ and $m_0=3$. There are two mirror-image curves: the first corresponding to a branch of optimal feedback schemes on which the detector loops are *wider* than the feedback coils, and the second to a branch on which the detector loops are *narrower* than the feedback coils. Thus, in region II there are a *wide range* of possible optimal designs (basically, any point on the curves shown in Fig. 4).

Figure 5(a) shows the mode coupling parameter, α_0, plotted as a function of the detector array radius, r_d, for a particular optimal $M=3$ feedback scheme in which $\Delta\theta_d=80°$ and $\Delta\theta_f=30°$ (i.e., moderate sized feedback coils,

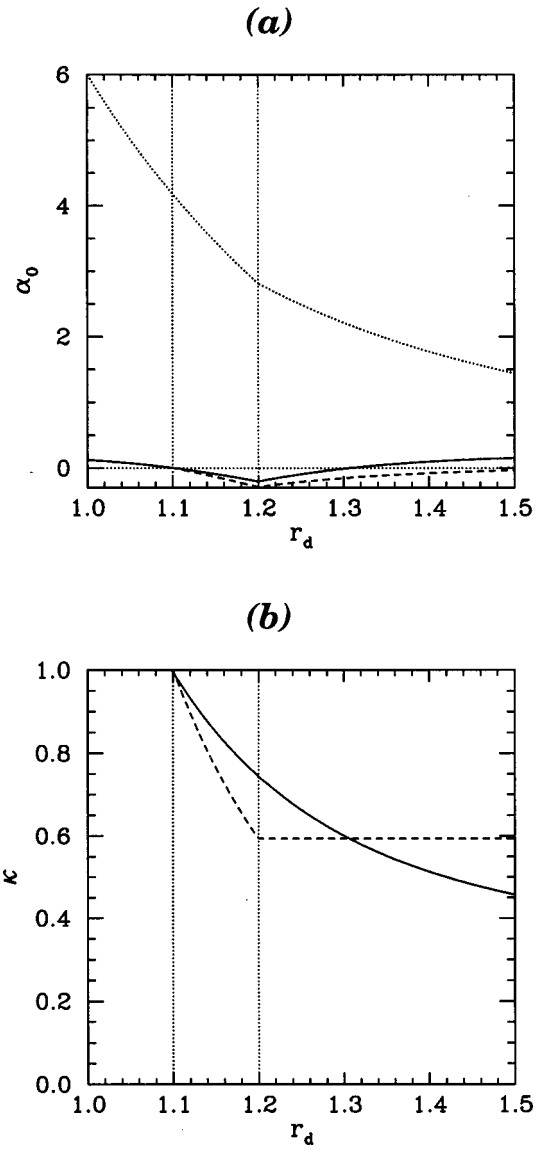

FIG. 5. (a) Values of α_0 (solid curve), $\alpha_{\max}$ (dotted curve), and $\alpha_{\min}$ (dashed curve), plotted as a function of r_d (divided by a), for $\Delta\theta_d=80°$, $\Delta\theta_f=30°$, $M=3$, $m_0=3$, $r_{m_0}=1.5a$, $r_w=1.1a$, and $r_f=1.2a$. The locations of the shell and the feedback coil array are indicated by vertical dotted lines. (b) The feedback efficacy parameter, κ, plotted as a function of r_d, for the same parameters as in (a). The dashed curve shows the κ vs r_d relation calculated assuming zero mode coupling.

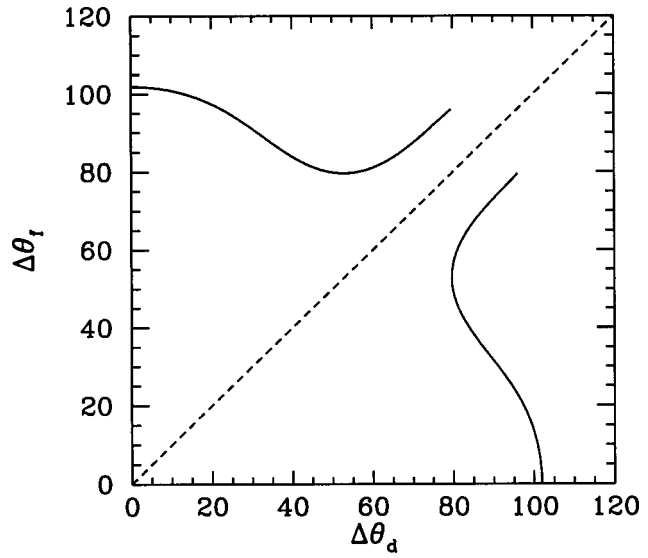

FIG. 6. Values of $\Delta\theta_f$ and $\Delta\theta_d$ (in deg) for which $\alpha_0=0$, calculated with $M=7$, $m_0=3$, $r_w=1.1a$, and $r_f=1.2a$.

and fairly large detector loops). Note that α_0 is zero when $r_d=r_w$, as expected, and remains fairly close to zero for other values of r_d. In other words, there is essentially *zero mode coupling* in this optimized scheme.

Figure 5(b) shows the feedback efficacy parameter, κ, plotted as a function of the detector array radius, r_d, for the optimal $M=3$ feedback scheme illustrated in Fig. 5(a). It can be seen that κ is rather large (i.e., about the same size as the corresponding parameter calculated in the absence of mode coupling—as is clear from the figure), reflecting the very low values of α_0 shown in Fig. 5(a). The largest value of κ (i.e., $\kappa=1$, which implies that the feedback-modified β limit is the same as the perfect-wall β limit) is obtained when $r_d \leqslant r_w$. All of the optimal schemes corresponding to the curves shown in Fig. 4 perform about as well as the scheme illustrated in Fig. 5.

We conclude that, in region II (i.e., $M=m_0$), there is a wide range of possible optimal feedback schemes. All schemes perform extremely well, i.e., they possess very low effective mode coupling. The optimum location for the detector loop array is *just outside* the shell, at which point the scheme performs with 100% efficiency (i.e., with $\kappa=1$). Note, in particular, that there is *no improvement in performance* when the detector array is placed inside the shell. Note, also, that all optimal schemes correspond to *nonoverlapping* feedback coils and detector loops.

Ideally, a practical feedback scheme should have zero effective mode coupling (such a scheme will perform with 100% efficiency when $r_d=r_w$), moderate sized, nonoverlapping, feedback coils (such coils will not take up too much space, and will be easy to support mechanically), and *large* detector loops (such loops will maximize the sensitivity of the scheme to low amplitude signals). As we have demonstrated, it is actually possible to find an optimal feedback scheme with just such properties in region II.

G. Region III: $M>2m_0$

In region III, it is also possible to set the mode coupling parameter, α_0, to zero when $r_d=r_w$. Figure 6 shows the loci of all points in $\Delta\theta_d-\Delta\theta_f$ parameter space at which $\alpha_0=0$, calculated for an example case in which $M=7$ and $m_0=3$. There are two mirror-image curves: the first corresponding to a branch of optimal feedback schemes on which the detector loops *overlap* and the feedback coils are *nonoverlapping*, and the second to a branch on which the detector loops are nonoverlapping and the feedback coils overlap. Thus, in region III there is again a *range* of possible optimal designs (i.e., most points on the curves shown in Fig. 6).

Figure 7(a) shows the mode coupling parameter, α_0, plotted as a function of the detector array radius, r_d, for a particular optimal $M=7$ feedback scheme in which $\Delta\theta_d$

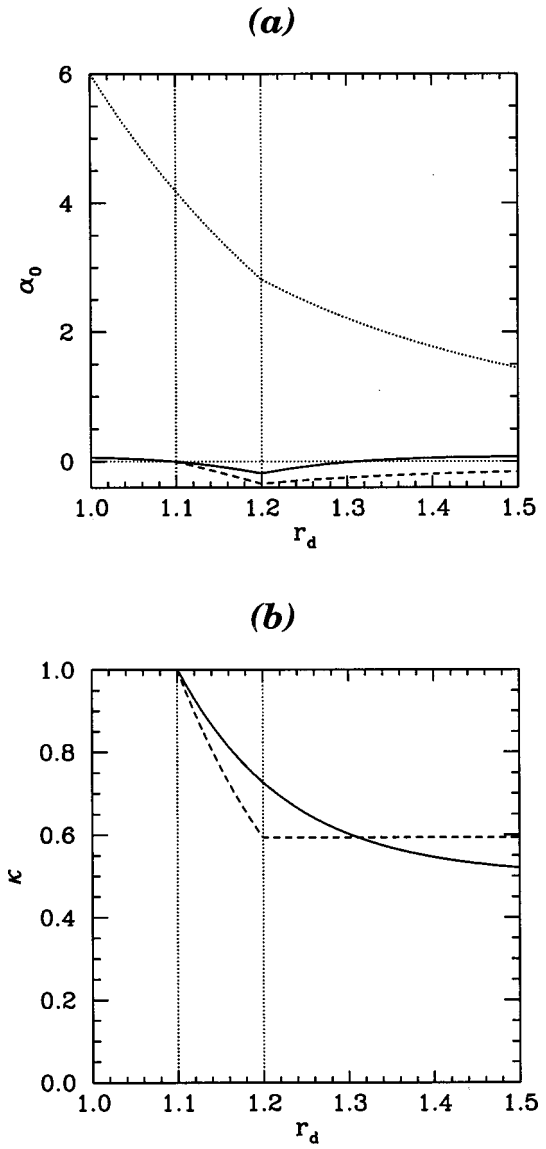

FIG. 7. (a) Values of α_0 (solid curve), $\alpha_{\max}$ (dotted curve), and $\alpha_{\min}$ (dashed curve), plotted as a function of r_d (divided by a), for $\Delta\theta_d=80°$, $\Delta\theta_f=50°$, $M=7$, $m_0=3$, $r_{m_0}=1.5a$, $r_w=1.1a$, and $r_f=1.2a$. The locations of the shell and the feedback coil array are indicated by vertical dotted lines. (b) The feedback efficacy parameter, κ, plotted as a function of r_d, for the same parameters as in (a). The dashed curve shows the κ vs r_d relation calculated assuming zero mode coupling.

$=80°$ and $\Delta\theta_f=50°$ (i.e., moderate sized, nonoverlapping feedback coils, and *overlapping* detector loops). Note that α_0 is zero when $r_d=r_w$, as expected, and remains fairly close to zero for other values of r_d. In other words, there is again essentially zero mode coupling in this optimized scheme.

Figure 7(b) shows the feedback efficacy parameter, κ, plotted as a function of the detector array radius, r_d, for the optimal $M=7$ feedback scheme illustrated in Fig. 7(a). It can be seen that κ is relatively large [i.e., about the same size as the corresponding parameter calculated in the absence of mode coupling—as is clear from Fig. 7(b)], reflecting the very low values of α_0 shown in Fig. 7(a). The largest value of κ (i.e., $\kappa=1$) is obtained when $r_d\leqslant r_w$. Most of the optimal schemes corresponding to the curves shown in Fig. 6 perform about as well as the scheme illustrated in Fig. 7. The only exceptions are schemes in which either the feedback coils or the detector loops are very small: such schemes perform badly.

We conclude that, in region III (i.e., $M>2m_0$), there is a fairly wide range of possible optimal feedback schemes. Most schemes perform extremely well, i.e., they possess very low effective mode coupling. The optimum location for the detector loop array is again just outside the shell, at which point the scheme performs with 100% efficiency (i.e., $\kappa=1$). As before, there is no improvement in performance when the detector array is placed inside the shell.

In region III, all optimal feedback schemes have either overlapping feedback coils or overlapping detector loops. Since overlapping feedback coils are considerably less practical than overlapping detector loops, the latter schemes are generally preferable.

H. Nonmode-specific feedback schemes

We have found two regimes in which it is possible to find an optimal feedback scheme which performs effectively with wide detector loops located just outside the shell. The first regime corresponds to $M=m_0$, whereas the second corresponds to $M>2m_0$. Unfortunately, the first regime is very *mode specific*. In other words, if $M=m_0$ for one particular value of m_0, then $M\neq m_0$ (and $M<2m_0$) for neighboring values. It follows that, in the first regime, a feedback scheme optimized for an $m_0=3$ resistive shell mode, say, is unlikely to perform effectively for $m_0=2$ or $m_0=4$ modes. In principle, the second regime is less mode specific than the first—after all, many values of m_0 simultaneously satisfy the inequality $M>2m_0$. In the following, we investigate the possibility of a nonmode-specific optimal feedback scheme in the second regime.

Figure 8 shows the loci of all points in $\Delta\theta_d-\Delta\theta_f$ parameter space at which $\alpha_0=0$, calculated for an example case in which $M=10$. Curves are displayed for $m_0=2$, 3, and 4. A nonmode-specific optimal feedback scheme would correspond to a mutual crossing point of these three sets of curves. Such a point does not exist. Note, however, that the three curves converge fairly closely in the regime where *both* the feedback coils and the detector loops overlap (i.e., in the upper-right quadrant of Fig. 8). Let us investigate this regime.

Figure 9 shows the feedback efficacy parameter, κ, plotted as a function of the detector array radius, r_d, for a nonmode-specific, optimal, $M=10$ feedback scheme (corresponding to the covergence point of the three sets of curves shown in Fig. 8) characterized by $\Delta\theta_d=38°$, $\Delta\theta_f=50.5°$, $r_w=1.1a$, and $r_f=1.2a$. Data are shown for $m_0=2$, 3, and 4. The scheme performs very well (i.e., with zero effective mode coupling) for $m_0=2$ and $m_0=3$, and slightly less well for $m_0=4$. Certainly, if the detector array were located just outside the shell then κ would be unity for $m_0=2$ and $m_0=3$, and would be about 0.83 for $m_0=4$ (i.e., the feedback modified β limit would be the perfect-wall β limit for $m_0=2$ and $m_0=3$, and would be 83% of the way between the no-wall and perfect-wall β limits for $m_0=4$). In this respect,

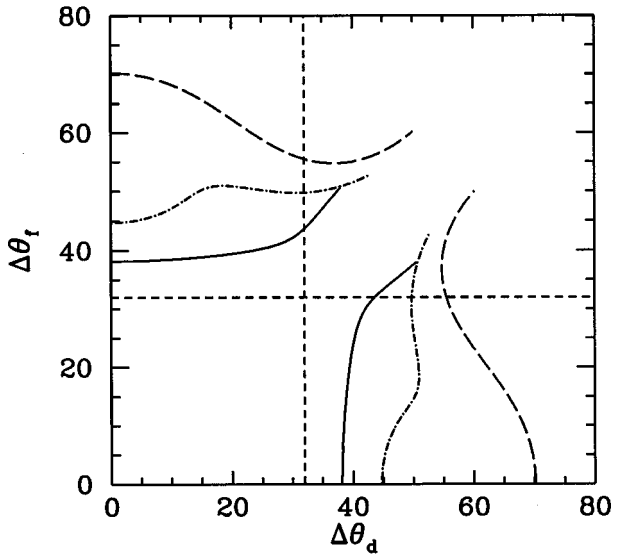

FIG. 8. Values of $\Delta\theta_f$ and $\Delta\theta_d$ (in deg) for which $\alpha_0=0$, for $M=10$, $r_w=1.1a$, and $r_f=1.2a$. The solid curves correspond to $m_0=2$, the dot-dashed curves correspond to $m_0=3$, and the long-dashed curves correspond to $m_0=4$. The short-dashed lines indicate the values of $\Delta\theta_f$ and $\Delta\theta_d$ above which the feedback coils and detector loops, respectively, start to overlap.

the scheme can be accurately described as being nonmode-specific. The scheme can either have strongly overlapping feedback coils and slightly overlapping detector loops, or vice versa. The former choice is probably more practical, since the conductors of slightly overlapping feedback coils are likely to get in one another's way.

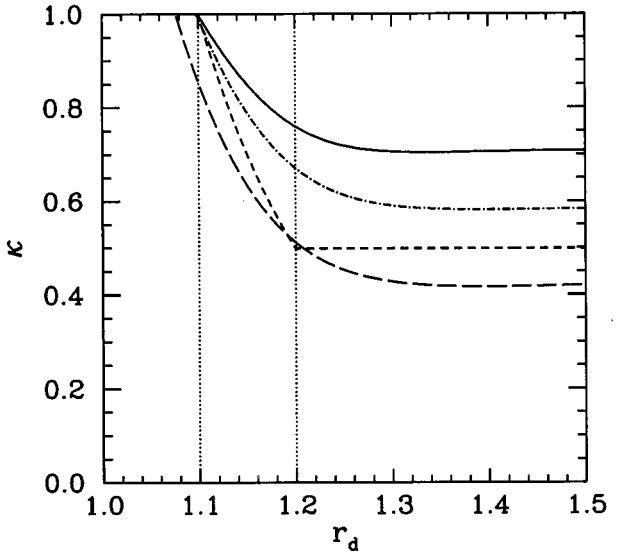

FIG. 9. The feedback efficacy parameter, κ, plotted as a function of r_d, for an optimal $M=10$ feedback scheme in which $\Delta\theta_d=38°$, $\Delta\theta_f=50.5°$, $r_w=1.1a$, and $r_f=1.2a$. The solid curve corresponds to $m_0=2$, the dot-dashed curve corresponds to $m_0=3$, and the long-dashed curve corresponds to $m_0=4$. The short-dashed curve shows the κ vs r_d relation calculated assuming zero mode coupling. The locations of the shell and the feedback coil array are indicated via vertical dotted lines.

V. SUMMARY

We have derived a quadratic dispersion relation, Eq. (61), which governs the feedback-modified stability of the resistive shell mode in a large-aspect ratio, low-β tokamak plasma. Our model feedback system allows for different sized feedback coils and detector loops in the poloidal direction, and also permits the feedback coil and detector loop arrays to be located at different minor radii.

The effectiveness of a given feedback scheme is governed by a parameter, α_0 [defined in Eq. (64)], which measures the coupling of different poloidal harmonics due to the nonsinusoidal nature of the feedback currents. The scheme fails completely if α_0 becomes either too positive (i.e., $\alpha_0>\alpha_{\max}$) or too negative (i.e., $\alpha_0<\alpha_{\min}$). The effectiveness criterion $\alpha_0<\alpha_{\max}$ is identical to the previously published criterion of Fitzpatrick and Yu (1998).[12] Moreover, the effectiveness criterion $\alpha_0>\alpha_{\min}$ is an extended version of the criteria of Boozer (1998)[13] and Okabayashi, Pomphrey, and Hatcher (1998).[14] Thus, the dispersion relation (61) succinctly *unifies* the apparently divergent elements of previous research. When the Fitzpatrick–Yu criterion is violated, the feedback scheme fails due to the distortion of the resistive shell mode eigenfunction generated by excessive mode coupling. Feedback fails when the Boozer–Okabayashi criterion is violated because the feedback system itself becomes unstable.

Using the dispersion relation (61), we find that feedback parameter space can be separated into *three* broad regions, depending on the nature and performance of the optimal feedback scheme. Let M be the number of feedback coils in the poloidal direction, and let m_0 be the poloidal mode number of the intrinsically unstable resistive shell mode.

Region I corresponds to $M\leqslant 2m_0$ and $M\neq m_0$. In this region, we find that the optimal feedback scheme is characterized by extremely narrow detector loops, which must be placed as close to the plasma as possible—in agreement with the work of Liu and Bondeson (2000).[15] Unfortunately, such a scheme is somewhat unfeasible, since, in practice, it would be almost impossible to mount detector loops well inside the resistive shell (especially in a reactor), and a scheme with very small detector loops is likely to have great difficulty sensing the resistive shell mode sufficiently early in its development for feedback to make a difference (since the signal to be detected has relatively long poloidal and toroidal wavelengths, whereas much of the background noise is short wavelength in nature).

Region II corresponds to $M=m_0$. In this region, it is possible to find an optimal feedback scheme with large, nonoverlapping detector loops, and moderately large, nonoverlapping feedback coils. The scheme operates with 100% efficiency (i.e., it effectively converts the resistive shell into a superconducting shell) when the detector loops are placed just outside the shell. There is no improvement in performance when the detector loops are placed inside the shell. Such a scheme is certainly practical (unlike the previous scheme). Unfortunately, it only operates effectively for one particular resistive shell mode (i.e., the mode whose poloidal mode number matches the number of feedback coils in the poloidal direction).

Region III corresponds to $M>2m_0$. In this region, it is possible to find an optimal feedback scheme with slightly overlapping detector loops, and strongly overlapping feedback coils. This scheme operates with close to 100% efficiency, for resistive shell modes with a *range* of different poloidal mode numbers, when the detector loops are placed just outside the shell. Obviously, such a scheme is not quite as practical as the previous one. On the other hand, it is far less mode specific.

VI. DISCUSSION

The main conclusion of this paper is that the principal failure mechanism for feedback systems designed to control the resistive shell mode in advanced tokamaks lies in the generation of sideband harmonic (i.e., harmonics other than the intrinsically unstable principal harmonic) magnetic fields by the nonsinusoidal currents flowing in the feedback coil array, and the subsequent detection and amplification of these fields by the feedback system. If the net sideband harmonic flux picked up by the detector loop array is too positive then feedback fails due to distortion of the resistive shell eigenfunction. If the net sideband harmonic flux is too negative then feedback fails because the feedback system becomes intrinsically unstable. The optimum feedback system corresponds to one in which the net sideband harmonic flux is *zero*. There are many ways to achieve this. One approach is to reduce the relative coupling between the feedback coil and detector loop arrays by making the detector loops very small, and locating them close to the plasma (and, hence, fairly far away from the feedback coils).[15] Another, more radical, approach is to reduce the coupling even further by making the detector loops measure the perturbed *poloidal* magnetic field, rather than the perturbed *radial* field.[23] The main problem with these two approaches is that they require small area detector loops, which are likely to have great difficulty picking up the resistive shell mode at low amplitudes, and only tend to work when the detector loops are located inside the shell, which is not reactor relevant. The approach adopted in this paper is quite different. We deal with feedback schemes in which there is *strong* coupling between the feedback coils and the detector loops. This allows the detector loops to be both large area and located outside the shell. However, we choose the poloidal widths of the individual feedback and detector loops to be such that the positive and negative components of the sideband harmonic flux picked up by the detector loop array *balance* one another, leading to zero net flux.

Although the analysis presented in this paper is restricted to cylindrical plasmas, it seems eminently plausible that the above-outlined approach to feedback design and optimization is also applicable to toroidal plasmas. However, this conjecture can only be verified via numerical simulations.

ACKNOWLEDGMENT

This research was funded by the U.S. Department of Energy, under Contract Nos. DE-FG05-96ER-54346 and DE-FG03-98ER-54504.

[1]The conventional definition of this parameter is $\beta=2\mu_0\langle p\rangle/\langle B^2\rangle$, where $\langle\cdots\rangle$ denotes a volume average, p is the plasma pressure, and B is the magnetic field strength.
[2]C. Kessel, J. Manickam, G. Rewoldt, and W. M. Tang, Phys. Rev. Lett. **72**, 1212 (1994).
[3]E. A. Lazarus, G. A. Navratil, C. M. Greenfield *et al.*, Phys. Rev. Lett. **77**, 2714 (1996).
[4]A. Bondeson, M. Benda, M. Persson, and M. S. Chu, Nucl. Fusion **37**, 1419 (1997).
[5]J. P. Goedbloed, D. Pfirsch, and H. Tasso, Nucl. Fusion **12**, 649 (1972).
[6]A. Bondeson and D. J. Ward, Phys. Rev. Lett. **72**, 2709 (1994).
[7]R. Betti and J. P. Freidberg, Phys. Rev. Lett. **74**, 2949 (1995).
[8]R. Fitzpatrick and A. Y. Aydemir, Nucl. Fusion **36**, 11 (1996).
[9]C. M. Bishop, Plasma Phys. Controlled Fusion **31**, 1179 (1989).
[10]R. Fitzpatrick and T. H. Jensen, Phys. Plasmas **3**, 2641 (1996).
[11]R. Fitzpatrick, Phys. Plasmas **4**, 2519 (1997).
[12]R. Fitzpatrick and E. P. Yu, Phys. Plasmas **5**, 2340 (1998).
[13]A. H. Boozer, Phys. Plasmas **5**, 3350 (1998).
[14]M. Okabayashi, N. Pomphrey, and R. E. Hatcher, Nucl. Fusion **38**, 1607 (1998).
[15]Y. Q. Liu and A. Bondeson, Phys. Rev. Lett. **84**, 907 (2000).
[16]C. Cates, M. Shilov, M. E. Mauel *et al.*, Phys. Plasmas **7**, 3133 (2000).
[17]R. C. Grimm, R. L. Dewar, J. Manickam, S. C. Jardin, A. H. Glasser, and M. S. Chance, in *Plasma Physics and Controlled Nuclear Fusion Research 1982*, Proceedings of the Ninth International Conference, Baltimore (IAEA, Vienna, 1983), Vol. 3, p. 35.
[18]J. Bialek, A. Boozer, M. Mauel, and G. Navratil, Bull. Am. Phys. Soc. **43**, 1831 (1998).
[19]J. Bialek (private communication).
[20]The standard large aspect-ratio ordering is $R_0/a\gg1$, where R_0 and a are the major and minor radii of the plasma, respectively.
[21]J. A. Wesson, Nucl. Fusion **18**, 87 (1978).
[22]R. Fitzpatrick, Phys. Plasmas **1**, 2931 (1994).
[23]T. S. Taylor (private communication).